Journal of Hazardous Materials 199–200 (2012) 367–374

Contents lists available at SciVerse ScienceDirect

Journal of Hazardous Materials

journal homepage: www.elsevier.com/locate/jhazmat

Synthesis of composite by application of mixed Fe, Mg (hydr)oxides coatings onto bentonite – A use for the removal of Pb(II) from water

M. Ranđelović[a,*], M. Purenović[a], A. Zarubica[a], J. Purenović[b], B. Matović[c], M. Momčilović[c]

[a] Department of Chemistry, Faculty of Science and Mathematics, University of Niš, 18000 Niš, Višegradska 33, Serbia
[b] Faculty of Electronic Engineering, University of Niš, 18000 Niš, A. Medvedeva 14, Serbia
[c] "Vinča" Institute of Nuclear Sciences, Belgrade University, P.O. Box 522, 11001, Serbia

ARTICLE INFO

Article history:
Received 30 May 2011
Received in revised form 17 October 2011
Accepted 7 November 2011
Available online 11 November 2011

Keywords:
Bentonite
Bentonite based composite
Pb(II) removal
Adsorption

ABSTRACT

The procedure for obtaining a bentonite based composite involves the application of mixed Fe and Mg hydroxides coatings onto bentonite particles in aqueous suspension and subsequent thermal treatment of the solid phase at 498 K. Structural and textural modifications of montmorillonite which occurred during the synthesis of composite were confirmed by XRD technique and N_2 adsorption at 77 K. The composite structure was found to be less ordered, while its specific surface area was about two times higher than the specific surface area of the starting/native bentonite. The effectiveness of the composite in Pb(II) removal from aqueous solutions at different initial concentrations, pH and ionic strengths of the solutions was examined. The equilibrium adsorption data were analyzed using three widely applied isotherms: Langmuir, Freundlich and Dubinin–Radushkevich. The composite effectively removes both ionic and colloidal forms of Pb(II) from water and the maximum adsorption capacity obtained from the Langmuir equation was 95.88 mg/g. The main mechanisms of Pb(II) removal at low pH values were ion-exchange and outer-sphere surface complexation.

1. Introduction

Lead (Pb) is heavy metal which presents one of the major environmental pollutants due to its hazardous nature. It diffuses into water and the environment through effluents from lead smelters as well as from battery, paper, pulp and ammunition industries. Scientists established that lead is nonessential for plants and animals, while for humans it is a cumulative poison which can cause damage to the brain, red blood cells and kidneys [1]. The greatest risk is to fetuses, babies and young children since it impedes their normal mental and physical development. According to the lead–copper rule, the U.S. EPA drinking water 90th percentile action level is 15 μg/dm^3. On average, it is estimated that lead in drinking water contributes to between 10 and 20% of total exposure (from all sources) [2]. For the purpose of environmental protection and public health, it is necessary to decrease the concentration of lead in contaminated water to the permissible limits before its discharge [3,4]. A wide variety of treatment processes can be used for the removal of Pb(II) from waters, and for certain, the cost plays an important role for determining which one is to be applied. The commonly methods used for the removal of Pb(II) from aqueous solutions include coagulation, sand filtration, ion-exchange, chemical precipitation, reverse osmosis, membrane processes, chemical oxidation or reduction and filtration [4,5]. However, all of the above mentioned techniques have significant disadvantages including incomplete metal removal, high consumptions of reagents and energy, low selectivity and generation of secondary wastes that are difficult to be disposed off [4]. Compared with other methods, adsorption technology has received much more attention because it has significant advantages including high efficiency in removing very low levels of heavy metals from dilute solutions, easy handling, high selectivity, lower operating cost, minimum production of chemical or biological sludge; it is convenient and economical for reducing trace quantities of heavy metals, etc. [4,6]. A number of adsorbent materials have been studied for their capacity to remove Pb(II), including activated carbon, zeolites, non-living biomass, clay minerals and other aluminosilicates [7].

Clay can be used as a depolluting agent due to its physical and chemical properties, i.e. large specific surface area, cation exchange capacity (CEC) and adsorptive affinity for inorganic and organic ions from water. Among the clays, bentonite is considered as a main candidate in the removal of lead and other heavy metal ions. Bentonite consists mostly of microcrystalline particles of montmorillonite which belongs to 2:1 clay minerals meaning that it has two tetrahedral sheets sandwiching a central octahedral sheet [8–11]. Since the existence of huge deposits of bentonite, there

* Corresponding author. Tel.: +381 64 2520599; fax: +381 18 533 014.
E-mail address: hemija@gmail.com (M. Ranđelović).

0304-3894/$ – see front matter © 2011 Elsevier B.V. All rights reserved.
doi:10.1016/j.jhazmat.2011.11.025

is a great potential for its utilization in wastewater treatment. In order to improve the physical and chemical properties of natural bentonites, such as adsorption capacity, special modification processes have been developed [12–15]. The heavy metals adsorption onto natural, Na^+-exchanged, acid activated or iron, aluminum and manganese oxide-coated adsorbents has received wide attention [12,16–20]. Some recent studies have reported effect of iron, magnesium and manganese oxide coatings on the removal of Pb(II) [14,15]. Eren [15] found that specific surface area of magnesium oxide coated bentonite is smaller than in the case of raw bentonite while iron oxide coating process leads to slightly increase of specific surface area. However, there is a lack of information how mixed iron/magnesium (hydr)oxides coatings affect structure, texture and adsorption characteristics of bentonite. Bearing in mind layered structure of montmorillonite, the quite limited extent of isomorphous substitution of Mg for Fe in iron (hidr)oxides and significant differences in acid–base surface properties between these two (hydr)oxides, formation of heterogeneous coatings onto bentonite and specific structure of obtained composite could be expected [21]. Different adsorption sites on such heterogeneous surface provide efficient removal of numerous chemical species of Pb(II) over a wide pH range.

In the present work, a cheap and effective composite material as a potentially attractive adsorbent for the treatment of Pb(II) contaminated water sources has been synthesized by coating of bentonite with mixed iron and magnesium (hydr)oxides (0.375 mmol Fe and 0.125 mmol Mg per gram of bentonite). Such synthesized material was characterized using the following techniques: XRD, ATR-FTIR, nitrogen adsorption isotherm – BET method and SEM. The adsorption efficacy of the composite material was investigated in the removal of Pb(II), by varying initial concentrations of Pb(II), pH, and ionic strength. The obtained results show that the composite has specific surface area twice the size compared to the native bentonite and efficiently removes Pb(II) from aqueous solutions over wide range of pH.

2. Materials and methods

2.1. Materials

The bentonite was supplied by Shenemil Co. (Serbia) with the following chemical composition (as oxide wt.%): 51.20 SiO_2, 26.86 Al_2O_3, 1.27 MgO, 2.30 Fe_2O_3, 1.44 CaO, 2.07 K_2O, 0.75 Na_2O, 0.10 MnO. The ignition loss of the bentonite at 1000 °C was found to be 15.26% and the cation exchange capacity determined by methylene blue method, was 54.75 meq/100 g. For the purpose of further composite synthesis, the native bentonite was purified and converted to Na^+-bentonite by treating with 1 M NaCl solution, as described elsewhere [22]. All reagents used in the experiments were of analytical grade.

2.2. Preparation of composite

The suspension containing 20 g of Na^+-bentonite in 400 cm^3 of distilled water was prepared and allowed to stand for 24 h. Subsequently, 100 cm^3 solution containing a mixture of $Fe(NO_3)_3 \times 9H_2O$ (3.03 g) and $Mg(NO_3)_2 \times 6H_2O$ (0.64 g) was added in small portions to vigorously stirred suspension; salts solution addition was done simultaneously with 0.5 M NaOH adding and maintaining the pH value of slurry within the range of 9–11. Finally, pH of slurry was adjusted to 10 and it aged for 12 h at room temperature. Then, the precipitate was filtered, washed using distilled water until there was no NO_3^- in filtrate and dried at 105 °C. At the end, the dried material was heated in a furnace at 498 K for 2 h. The structure of the composite is stabilized by thermal treatment at 498 K resulting in low water swelling characteristic and can be easily separated by filtration or centrifuging, in contrast to native bentonite. Thus, during thermal treatment the composite loses only adsorbed water, while structural –OH groups are not removed and can act as adsorption sites [21].

For the experiments in this study the composite was finely powdered in an agate mortar and passed through a 120 mesh sieve (particles size less than 125 μm).

2.3. Characterization

The native bentonite and the composite were characterized using the following techniques under conditions described in further text. Attenuated Total Reflectance Fourier Transform Infrared (ATR-FTIR) spectra were recorded on an ATR-FTIR spectrometer Bruker Tensor-27 equipped with MCT detector in the region 4000–400 cm^{-1}. XRD patterns were taken by the use of a Siemens D500 diffractometer with a Ni filter using Cu Kα radiation (λ = 0.154 nm) and the step-scan mode with a step width of 0.02° and 1 s/step. Scanning electron microscopy (SEM) was performed on a JEOL JSM-5300. Surface areas were measured by adsorption of N_2 at 77 K using Sorptomatic 1990 Thermo Scientific and the calculation was carried out with a molecular area of 16.2 $Å^2$. Prior to the surface area measurements, each sample was outgassed at room temperature for 4 h and then 18 h at 110 °C. The specific surface area was calculated by the BET equation. The micropore volume was evaluated by the method of Dubinin–Radushkevich, and the mesopores size distribution was determined using the Barrett–Joyner–Halenda (BJH) method. Zeta potential (ZP) and particle size measurements were performed by Dynamic Light Scattering (DLS) technique using a Zeta-sizer Nano ZS with 633 nm He–Ne laser and 173° detection optics (Malvern, UK). Measurement uncertainty is given as standard deviation of average ZP or particle size value for ten consecutive runs.

The surface charge of composite was estimated by measuring NH_4^+ and Cl^- retention at pH 7 according to the following procedure. One gram of air-dried composite was placed in polyethylene centrifuge tube and 40 cm^3 of 1 M NH_4Cl was added. The sample was stirred for 2 h and centrifuged. The supernatant was discarded and the amount of 40 cm^3 of 0.5 M NH_4Cl was then added followed by 12 h of stirring, centrifugation and supernatant removal. The washing procedure was carried out with 40 cm^3 of 0.01 M NH_4Cl. Three washes were preformed with stirring for 30 min between washes. After the final wash the supernatant was discarded and polyethylene tube weighted to compensate for entrained NH_4Cl solution. Retained NH_4^+ and Cl^- were displaced by three washings with 1 M of $NaNO_3$. The extracts were combined and diluted to 250 cm^3. The concentration of NH_4^+ and Cl^- were corrected for entrained NH_4Cl solution and used for the amount of positive and negative surface charges determination.

2.4. Retention experiments

The adsorption experiments were carried out by the batch equilibrium technique at 20 °C. The lead stock solution (1000 mg/dm^3) was prepared by dissolving the required amount of $Pb(NO_3)_2$ in distilled water. In the adsorption isotherm experiments the initial concentration of Pb(II) was in the range from 30 to 120 mg/dm^3 and the adsorbent dosage was 1 g/dm^3. The initial pH values were adjusted at 4.0 ± 0.1. After the suspensions were equilibrated for 120 min, liquid and solid phases were separated. Residual Pb(II) concentrations were determined using the Atomic absorption spectrometer Perkin Elmer Analyst 300. After the adsorption experiments the composite was collected, dried at room temperature and analyzed by ATR-FTIR.

The adsorption of Pb(II) on bentonite composite was also examined in the background electrolyte solutions of 0.005, 0.01, 0.05, and 0.1 M $NaNO_3$ and at the pH values ranging from 2.0 to 12.0. The adjustment of pH value was carried out by the addition of 0.1 M and 0.01 M HNO_3 or NaOH.

2.5. Theoretical approach

The adsorption capacity (q_e) of Pb(II) (mg/g) was calculated using the equation

$$q_e = \frac{V(C_0 - C_e)}{m_{ads}} \quad (1)$$

where V is the volume of Pb(II) solution (dm^3), C_0 is the initial concentration of the Pb(II) solution (mg/dm^3), C_e is the equilibrium concentration of the Pb(II) solution (mg/dm^3) and m_{ads} is the mass of adsorbent (g).

In this study, the equilibrium experimental data for adsorption of Pb(II) on the composite were analyzed using the Langmuir, Freundlich and Dubinin–Radushkevich (D–R) isotherm models [23–25]. These isotherms were used in the linear forms as follows:

The linear form of Langmuir isotherm can be represented by the following equation:

$$\frac{C_e}{q_e} = \frac{1}{K_L} + \frac{a_L}{K_L} C_e \quad (2)$$

K_L (dm^3/g) is the Langmuir equilibrium constant, and a_L (dm^3/mg) is the Langmuir constant related to the energy of adsorption. The K_L/a_L gives the theoretical monolayer saturation capacity, Q_0. R_L is a dimensionless constant known as the separation factor which is defined by the following equation:

$$R_L = \frac{1}{1 + a_L C_0} \quad (3)$$

The linear form of Freundlich isotherm is:

$$\log\ q_e = \log K_F + \frac{1}{n} \log C_e \quad (4)$$

In which K_F ($mg^{1-1/n}\ dm^{3/n}/g$) represents the adsorption capacity when the metal ion equilibrium concentration equals to 1, and n represents the degree of dependence of the adsorption on equilibrium concentration.

The linearized D–R equation has the following form:

$$\ln\ q_e = \ln q_m - \beta\varepsilon^2 \quad (5)$$

where q_e is adsorption capacity (mol/g), q_m is the maximum adsorption capacity, i.e. the amount of metal ions at complete monolayer coverage (mol/g), β is the activity coefficient related to mean adsorption energy (mol^2/kJ^2), and ε is the Polanyi potential ($\varepsilon = RT \ln(1 + 1/C_e)$). The value of β is related to the adsorption free energy, E (kJ/mol), which is defined as the free energy change required to transfer 1 mol of ions from solution to the solid surfaces. The relation is as the following equation:

$$E = \frac{1}{\sqrt{-2\beta}} \quad (6)$$

3. Results and discussion

3.1. XRD and SEM results

The XRD patterns of the composite, starting (native) bentonite and bentonite calcined at 1123 K are presented in Fig. 1a–c, respectively.

The positions of d_{001}, d_{003}, $d_{020-110}$, $d_{130-200}$ and d_{060} peaks of native bentonite are observed at 5.74, 17.30, 19.88, 34.88, 61.93 (2θ) and the corresponding peaks of the composite are at 6.90, 17.60, 19.87, 34.95, 61.85 (2θ). Non-clay minerals such as quartz and cristobalite are included in the composition of bentonite as well as the composite. The peaks originating from d_{100} and d_{101} quartz diffractions are seen at 20.86 and 26.64 (2θ), respectively, and cristobalite peak corresponding to d_{101} diffraction is observed at 21.84 (2θ). After the calcination of bentonite at 1123 K, the peaks corresponding to montmorilonite disappeared. However, peaks derived from quartz and cristobalite, which were covered with the peaks of montmorillonite, can be clearly seen in Fig. 1c. The structural changes of montmorillonite are mainly reflected in the reduction of d_{001} diffraction peak intensity and its shifting towards the higher values of 2θ. Moreover, it is observed that the peak is broadened suggesting that the distance between the layers is non-uniform with disordered and partially delaminated structure. The crystallographic spacing d_{001} of montmorillonite in the native bentonite and the composite, computed by using Bragg's equation ($n\lambda = 2d \sin\theta$), is 1.54 nm and 1.28 nm, respectively. These changes

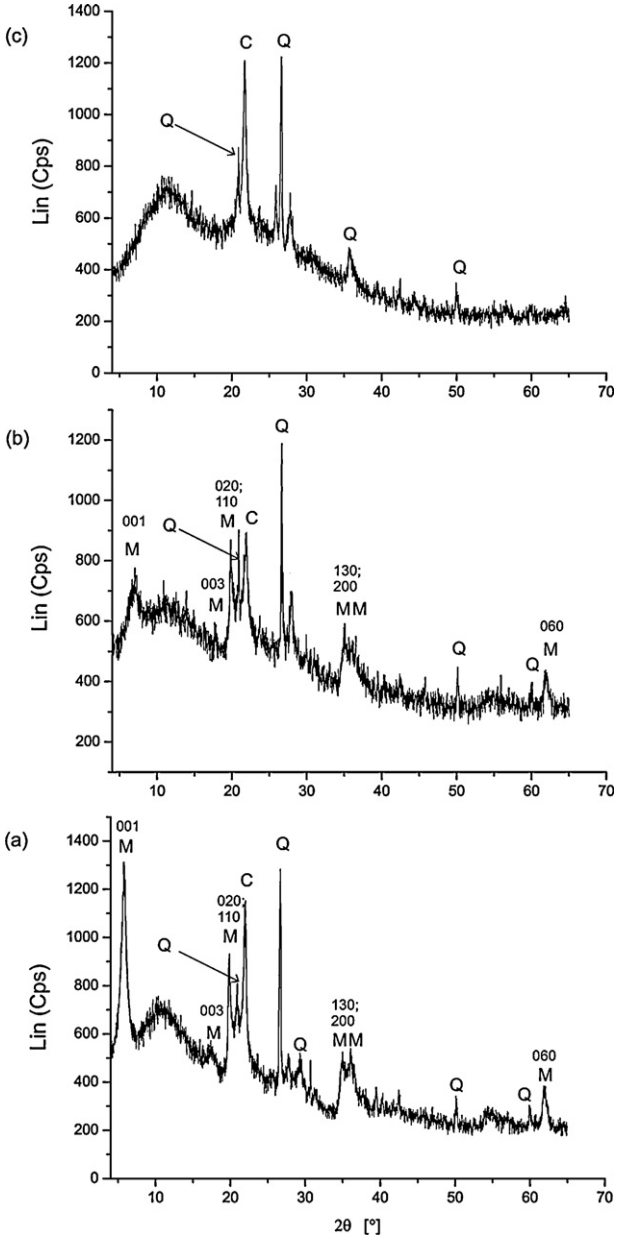

Fig. 1. X-ray diffractograms of (a) composite, (b) native bentonite and (c) bentonite calcined at 1123 K.

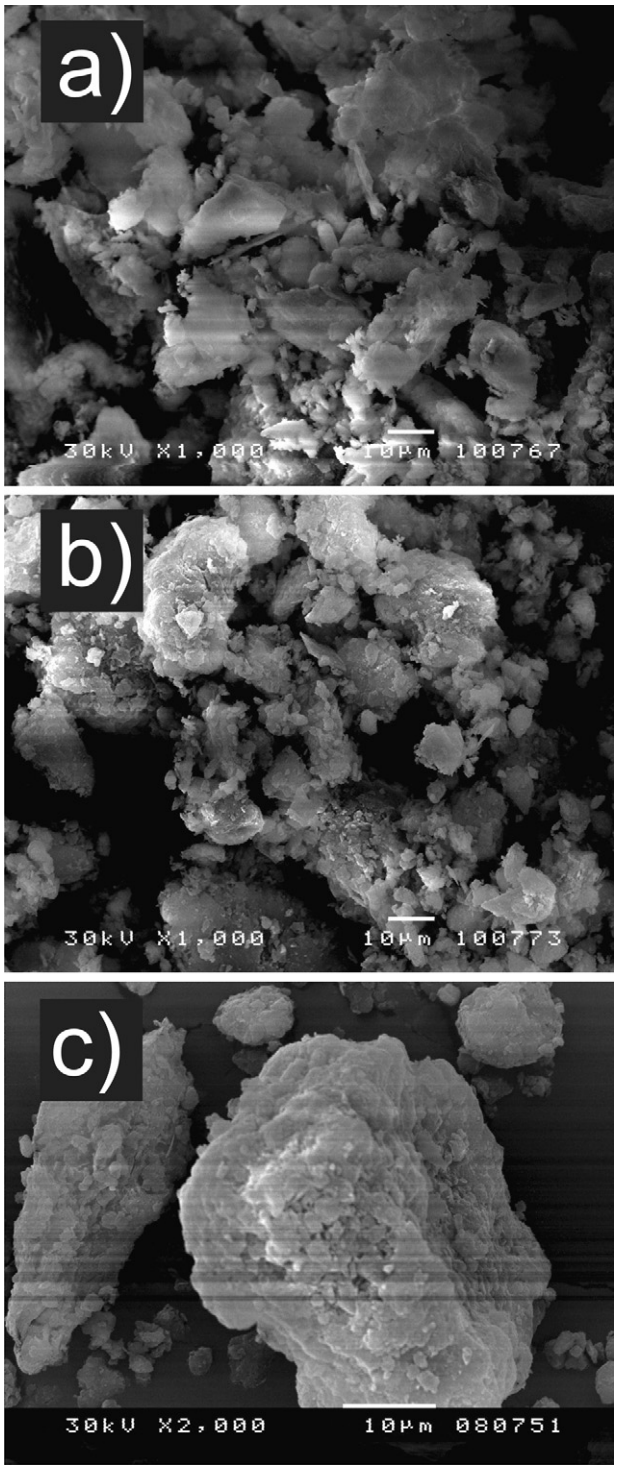

Fig. 2. (a) SEM of synthesized composite, (b) SEM of composite after interaction with Pb(II) solution and (c) surface morphology of the native bentonite.

in the structure took place because the d-spacing is very sensitive to the type of interlamellar cations, and the degree of their hydration [10].

SEM micrographs (Fig. 2a–c) show that bentonite and composite are composed of laminar particles arranged in layered manner, forming the aggregates with diameters up to 50 μm.

No significant changes in the microstructure of composite occurred during the interaction with the aqueous solution of Pb(II).

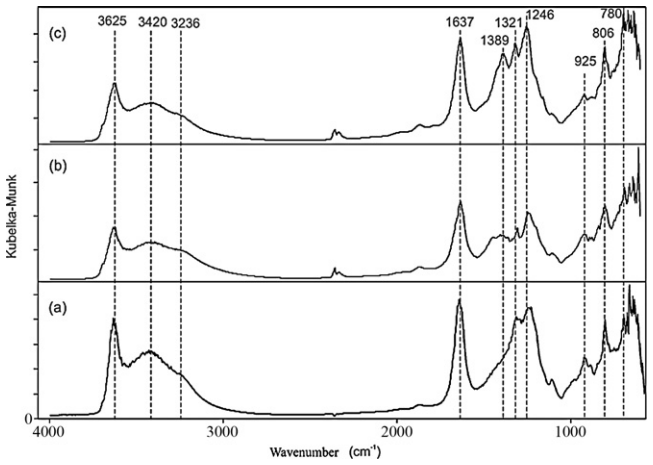

Fig. 3. ATR-FTIR spectra of (a) bentonite, (b) composite after the interaction with Pb(II) solution and (c) composite before the interaction with Pb(II) solution.

3.2. ATR-FTIR spectral data, surface charge and cation exchange properties

The ATR-FTIR spectra of native bentonite and composite before and after the interaction with Pb(II) solution were presented in Fig. 3.

The OH stretching vibrations which originate from the Al–Al–OH stretches are observed at 3625 cm^{-1}. The envelope at 3420 cm^{-1} belongs to the OH stretching of H-bonded water, with a shoulder near 3236 cm^{-1}, due to the overtone of the bending vibration of water observed at 1637 cm^{-1}. A vibration mode at ca. 1389 cm^{-1} is attributed to the NO_3^- stretching mode. Despite a thorough washing process, a large amount of NO_3^- is retained in the composite. The occurrence of NO_3^- indicates that some positive charged sites exist on the surface of composite and that they are counterbalanced by the NO_3^- which can be exchanged by other anions. In addition, the formation of poorly crystallized magnesium hydroxonitrate in pH range 9–11 [26,27], where Fe/Mg coprecipitation was performed over bentonite particles, is very likely. The bends at 1331 cm^{-1} and 1246 cm^{-1} are due to Si–O bending vibrations. The additional bend corresponding to Al–Al–OH is observed at 925 cm^{-1}. A bend at 806 cm^{-1} with inflexion at 780 cm^{-1} confirms quartz admixture.

The results obtained from NH_4Cl adsorption method indicate that the negative and positive charge at the composite surface is 0.5123 mmol/g and 0.0137 mmol/g, respectively.

3.3. Specific surface area determined by N_2 adsorption/desorption using BET equation

Fig. 4 shows the comparative nitrogen adsorption–desorption isotherms of bentonite and composite.

The isotherms can be assigned to Type II isotherms, corresponding to non-porous or macroporous adsorbents. The hysteresis loops of Type H3 in the IUPAC classification occur at $p/p^0 > 0.5$, which is not inside the typical BET range. Furthermore, hysteresis loops of these isotherms indicate that they were given by either slit-shaped pores or, as in the present case, assemblages of platy particles of montmorillonite. Porous structure parameters are summarized in Table 1.

Compared to native bentonite, during the composite synthesis additional meso- and micropores were generated. Pore volumes (Gurvich) at p/p^0 0.999 for bentonite and composite are 0.180 cm^3/g and 0.243 cm^3/g, respectively. It was found that isotherms gave

Table 1
Surafce area and porosity of native bentonite and composite, determined by applying BET, BJH and D–R equation to N_2 adsorption at 77 K.

Sample	S_{BET} (m^2/g)	Median mesopore diameter (nm)	Cumulative mesopore area (m^2/g)	Cumulative mesopore volume (cm^3/g)	Micropore volume (cm^3/g)
Bentonite	37.865	13.629	53.329	0.1202	0.0153
Composite	80.385	11.021	82.675	0.1716	0.0316

linear BET plots from p/p^0 0.03 to 0.21 for bentonite and from 0.03 to 0.19 for composite.

The composite has the specific surface area that is twice the size compared to the surface area of the native bentonite. This can be explained by the structural changes that occurred during the chemical and thermal modification of the native bentonite. The structural changes include delamination as well as the decrease of the distance between the layers of montmorillonite particles, because the interlayer water was lost under heating. The higher surface area of composite mainly results from the interparticle spaces generated by the three-dimensional co-aggregation of magnesium polyoxocations, iron oxide clusters and plate particles of montmorillonite. Macro- and mesopores arose from particle-to-particle interactions, while micropores were generated in the interlayer spaces of clay minerals due to irregular stacking of layers of different lateral dimensions [28].

It is apparent that the changes of montmorillonite structure are responsible for the creation of new pore structure in the composite, which is then stabilized by the thermal treatment with the removal of H_2O molecules. The changes that involve partial dehydroxylation and cationic dehydration are brought about by thermal activation and they lead to various forms of cross-linking between oxides and smectite framework. As a result, composite does not swell and can be easily separated from water by filtration or centrifugation. There is a wide pore size distribution which supports disordered structure consisting of the delaminated parts with mesoporosity and the layered parts with microporosity.

3.4. Pb(II) adsorption

The effect of contact time on the adsorption of Pb(II) by composite is shown in Fig. 5 for the initial pH values of 2.7 and 4.0. It is interesting to note that the removal percentage of Pb(II) on the composite at both pH values sharply achieves a highest value at the beginning of adsorption process. Then the amount of adsorbed Pb(II) decreased with the increase in contact time and adsorption process almost completely reached the equilibrium after 40 min.

The adsorption data were fitted by Langmuir, Freundlich, and D–R models (Fig. 6a–c), since the process was complex and it included various physical and chemical interactions. The linear equation parameters were determined by using the Origin 7 software (Table 2).

Langmuir model serves to estimate the complete monolayer adsorption capacity. It is found that the complete monolayer adsorption capacity of the composite is 95.88 mg/g. Value of R_L which is in the range 0–1 (Table 2), confirms the favorable adsorption process of the Pb(II).

Freundlich model is important because it assumes heterogeneous surface. According to the literature, when $n > 1$, the adsorption is favorable [5]. The higher the n value means stronger adsorption intensity. In this study, Pb(II) adsorption isotherm shows that adsorption of Pb(II) onto composite is favorable since n value is 3.35. The K_F value of the Freundlich equation (Table 2) also indicates that the composite has a very high adsorption capacity for Pb(II) ions in aqueous solutions. As stated in the literature, the E value of Dubinin–Radushkevich equation ranges from 1.0 to 8.0 kJ/mol for physical adsorption and from 8.0 to 16.0 kJ/mol for chemical ion exchange adsorption [5]. Hence, it is possible to say that the adsorption mechanism of Pb(II) on the composite can be explained with an ion exchange process. The Dubinin–Radushkevich equation has shown a better fit to experimental data than Freundlich equation, but the best fit is in the case of Langmuir equation. The maximum Pb(II) ion adsorption capacity, Q_0, in the present study was compared with the other adsorbents reported in the literature (Table 3).

Ion exchange of Mg^{2+} with Pb^{2+} ions was confirmed by measuring the magnesium concentrations after contacting of composites with distilled water and Pb(II) solutions at initial pH of 4. After the interaction of the composite with distilled water, the concentration of magnesium was 0.250 mg/dm^3. On the contrary, during the composite interaction with Pb(II) solution of 120 mg/dm^3, much greater amount of magnesium was released into the water and its concentration was 2.651 mg/dm^3. Therefore, the process of Pb(II) removal by the composite leads to the lowering of Pb(II) concentration and

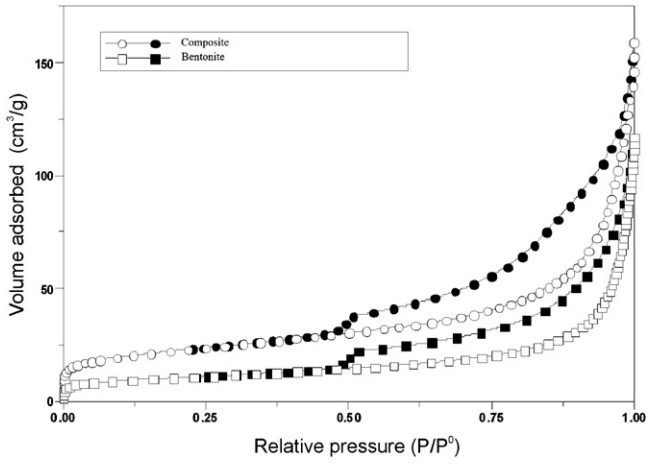

Fig. 4. Nitrogen adsorption–desorption isotherms of native bentonite and composite.

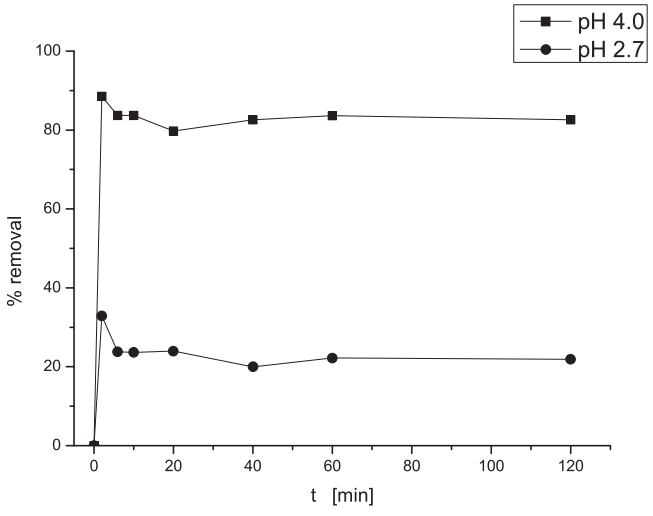

Fig. 5. Effect of contact time on the adsorption of Pb(II) on the composite.

Table 2
The parameters for Langmuir, Freundlich and D–R isotherms.

Langmuir					Freundlich			D–R		
K_L (dm^3/g)	α_L (dm^3/mg)	Q_0 (mg/g)	R_L /	r^2 /	K_F ($mg^{1-1/n}\,dm^{3/n}/g$)	n /	r^2 /	E kJ/mol	q_m (mg/g)	r^2 /
39.00	0.407	95.88	0.020–0.076	0.997	35.19	3.35	0.923	8.45	108.82	0.967

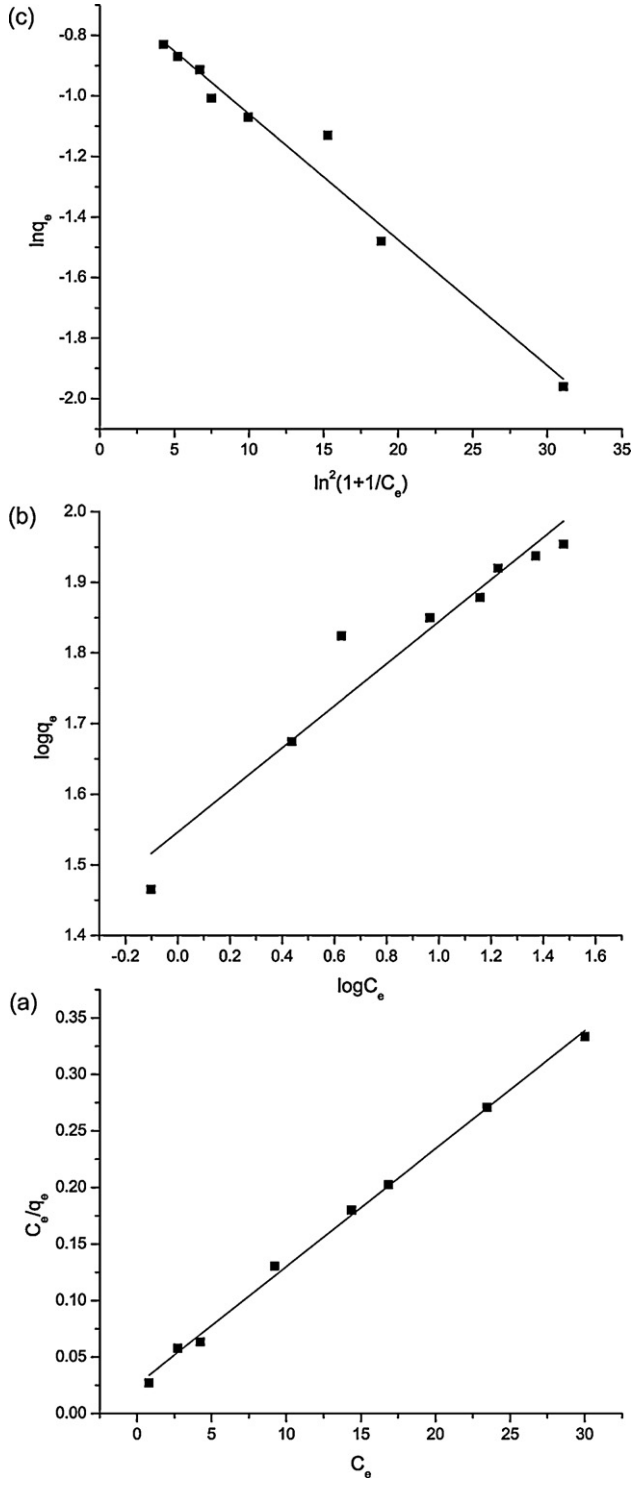

Fig. 6. (a) Langmuir isotherm, (b) Freundlich isotherm and (c) D–R isotherm plot of Pb(II) adsorption on the composite.

water enriched with magnesium which is important and valuable element for good human health.

The pH of the Pb(II) solution plays an important role in the adsorption process, influencing not only the surface charge of the adsorbent and the dissociation of functional groups on the active sites of the adsorbent but also the solution Pb(II) chemistry. The adsorption of Pb(II) on the composite decreased when pH decreased as shown in Fig. 7a.

The adsorptive decrease at pH below 5 was caused by the competition between H^+ and Pb^{2+} for the negatively charged surface sites. Maximum retention is in the pH range 5–10. The main Pb(II) species in the pH range 6.5–10 are $Pb(OH)^+$ and $Pb(OH)_2$ which can easily form colloidal micelles characterized with the following imposed structure:

$$\{m[Pb(OH)_2]nPb(OH)^+\cdot(n-x)NO_3^-\}xNO_3^- \quad (7)$$

The potential-determining ion is $Pb(OH)^+$ and that is the reason for the positive ZP of colloidal Pb(II) at the pH below 10 [36,37]. Therefore, colloidal micelles were easily attracted by the negatively charged composite surface. Particle size of colloidal Pb(II) at pH 7 ± 0.1 was determined to be 268.7 ± 16.7 nm. At the pH range of 10–12 the predominant Pb(II) species are $Pb(OH)_2$ and $Pb(OH)_3^-$ which give rise to the formation of negatively charged colloidal micelles with the following structure:

$$\{m[Pb(OH)_2]nPb(OH)_3^-\cdot(n-x)Na^+\}xNa^+ \quad (8)$$

ZP values for Pb(II) colloidal solutions at pH 11.8 were -50.7 ± 3.6 mV with particle size of 252.7 ± 28.2 nm. Having in mind surface heterogeneity of the composite and high point of zero charge value of $Mg(OH)_2$ (between pH 12 and pH 13) [38], negative ions and particles can be adsorbed on the positively charged surface sites at pH 10–12. Removal efficiency of $Pb(OH)_3^-$ was higher than negatively charged colloids, probably because the ionic species were involved in the process of ion exchange and chemisorption, while colloidal micelles could be bound to the surface dominantly by electrostatic forces.

The increase in salt concentration decreased the Pb(II) removal efficiency (Fig. 7b). With the increase of ionic strength, the adsorption capacity decreased due to the screening of composite surface charges. The adsorption process that depends on ionic strength

Table 3
Adsorption results of Pb(II) by various adsorbents from the literature.

Adsorbent	Adsorption capacity (mg/g)	Ref. No.
Expanded perlite	13.39	[5]
Activated alumina	83.33	[29]
Mustard husk	30.48	[30]
MX-80 bentonite	68.58	[31]
Coconut-shell carbon	26.51	[32]
GMZ bentonite	23.83	[11]
Pine cone activated carbon	27.53	[33]
Clinoptilolite	80.93	[34]
Fallen *Cinnamomum camphora* leaves, at 303.2 K	73.15	[35]
Iron oxide coated bentonite	22.20	[15]
Magnesium oxide coated bentonite	31.86	[15]
Bentonite based composite	95.88	In this study
Bentonite	68.84	In this study

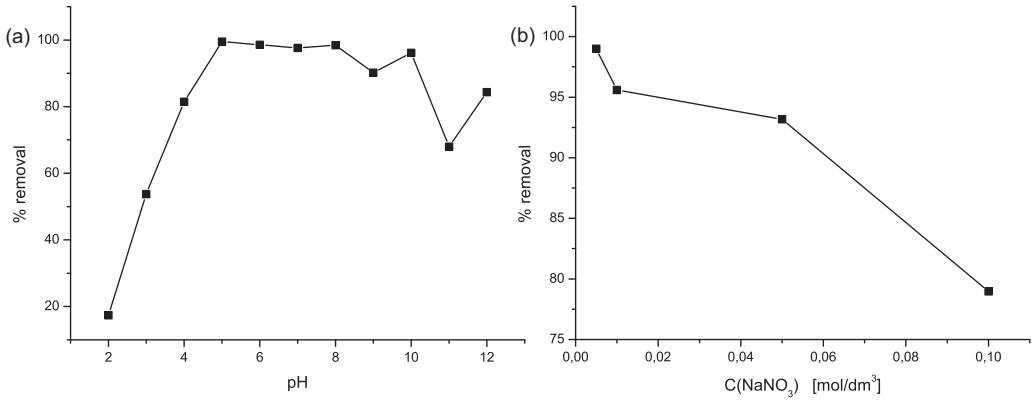

Fig. 7. Effect of (a) pH and (b) $NaNO_3$ concentration on adsorption of Pb(II) onto composite.

of the solution is consistent with the previously assumed ion exchange mechanism. Outer-sphere surface complexes are more sensitive to ionic strength variations than inner-sphere complexes because the background electrolyte ions are placed in the same plane as Pb^{2+} in outer-sphere surface complexes. Therefore, it can be deduced that cation-exchange and/or outer sphere surface complexation mainly contribute to Pb(II) adsorption on the composite in the acidic pH region. Inner-sphere surface complexation includes the formation of Pb polymers and could be the main adsorption mechanism of Pb(II) at pH > 7 [3,11,39,40].

4. Conclusion

Simple procedure of iron and magnesium hydroxides layering on the bentonite matrix brought significant changes in the structure and texture of montmorillonite, which is the predominant clay mineral of bentonite. During the synthesis, partially delaminated and less ordered structure was obtained, which resembles the house of cards. Thermal treatment led to the dehydration of surface and interlamellar area resulting in the increase of specific surface area and microporosity, compared to the starting bentonite.

The Langmuir model fits adsorption isotherm better than Freundlich and D–R model. Composite effectively removed ionic and colloidal forms of Pb(II), with the greatest efficiency in the pH range of 5–10. The explanation lies in the fact that reducing the pH below 5 causes the surface protonation, i.e. there was a competitive process of protons and Pb(II) ions adsorption. The pH increase led to the formation of colloidal forms of lead, which were more or less bound to the surface of the composite, depending on the type of charge that colloidal micelles carried.

At pH 12 soluble form of lead $Pb(OH)_3^-$ was removed from water very well. The main mechanism of lead removal is ion exchange, but formation of outer- and inner-sphere complexes is also possible. With the increase of ionic strength of solution, the percentage removal of lead was reduced, because the negative charge on the surface was screened by Na^+ ions. Bearing in mind the results obtained in this study, it can be concluded that the composite shows a high adsorption affinity for Pb(II) in water and it can be applied for purification of contaminated aqueous media that contain Pb(II) in high concentrations.

Acknowledgement

This study was financially supported by the Ministry of Science and Technological Development of the Republic of Serbia, through Project TR19031.

References

[1] Lead in Drinking-water, Background Document for Development of WHO Guidelines for Drinking-water Quality, World Health Organization, 2003.
[2] Lead and Copper Rule A Quick Reference Guide for Schools and Child Care Facilities that are Regulated Under the Safe Drinking Water Act, Office of Water, EPA, 2005.
[3] S.T. Yang, D.L. Zhao, H. Zhang, S.S. Lu, L. Chen, X.J. Yu, Impact of environmental conditions on the sorption behavior of Pb(II) in Na-bentonite suspensions, J. Hazard. Mater. 183 (2010) 632–640.
[4] D. Ozdes, A. Gundogdu, B. Kemer, C. Duran, Removal of Pb(II) ions from aqueous solution by a waste mud from copper mine industry: equilibrium, kinetic and thermodynamic study, J. Hazard. Mater. 166 (2009) 1480–1487.
[5] A. Sari, M. Tuzen, D. Citak, M. Soylak, Adsorption characteristics of Cu(II) and Pb(II) onto expanded perlite from aqueous solution, J. Hazard. Mater. 148 (2007) 387–394.
[6] S.T. Yang, J.X. Li, D.D. Shao, J. Hu, X.K. Wang, Adsorption of Ni(II) on oxidized multi-walled carbon nanotubes: effect of contact time, pH, foreign ions and PAA, J. Hazard. Mater. 166 (2009) 109–116.
[7] P. King, N. Rakesh, S. Beenalahari, Y. Prasanna Kumar, V.S.R.K. Prasad, Removal of lead from aqueous solution using *Syzygium cumini* L.: equilibrium and kinetic studies, J. Hazard. Mater. 142 (2007) 340–347.
[8] H.H. Murray, Traditional and new applications for kaolin, smectite, and palygorskite: a general overview, Appl. Clay Sci. 17 (2000) 207–221.
[9] Z. Orolinova, A. Mockovčiakova, Structural study of bentonite/iron oxide composites, Mater. Chem. Phys. 114 (2009) 956–961.
[10] B. Caglar, B. Afsin, A. Tabak, E. Eren, Characterization of the cation-exchanged bentonites by XRPD, ATR, DTA/TG analyses and BET measurement, Chem. Eng. J. 149 (2009) 242–248.
[11] S. Wang, Y. Dong, M. He, L. Chen, X. Yu, Characterization of GMZ bentonite and its application in the adsorption of Pb(II) from aqueous solutions, Appl. Clay Sci. 43 (2009) 164–171.
[12] M. Hajjaji, H. El Arfaoui, Adsorption of methylene blue and zinc ions on raw and acid-activated bentonite from Morocco, Appl. Clay Sci. 46 (2009) 418–421.
[13] B. Benguella, A. Yacouta-Nour, Adsorption of Bezanyl Red and Nylomine Green from aqueous solutions by natural and acid-activated bentonite, Desalination 235 (2009) 276–292.
[14] E. Eren, Investigation of a basic dye removal from aqueous solution onto chemically modified Unye bentonite, J. Hazard. Mater. 166 (2009) 88–93.
[15] E. Eren, Removal of lead ions by Unye (Turkey) bentonite in iron and magnesium oxide-coated forms, J. Hazard. Mater. 165 (2009) 63–70.
[16] W.H. Kuan, S.L. Lo, M.K. Wang, C.F. Lin, Removal of Se(IV) and Se(VI) from water by aluminum-oxide-coated sand, Water Res. 32 (3) (1998) 915–923.
[17] R. Han, W. Zou, Z. Zhang, J. Shi, J. Yang, Removal of copper(II) and lead(II) from aqueous solution by manganese oxide coated sand: I. Characterization and kinetic study, J. Hazard. Mater. B137 (2006) 384–395.
[18] V.K. Gupta, V.K. Saini, N. Jain, Adsorption of As(III) from aqueous solutions by iron oxide-coated sand, J. Colloid Interface Sci. 288 (2005) 55–60.
[19] M.W. Wana, C.C. Kan, B.D. Rogel, M. Lourdes, P. Dalida, Adsorption of copper (II) and lead (II) ions from aqueous solution on chitosan-coated sand, Carbohydr. Polym. 80 (2010) 891–899.
[20] S.G. Wang, W.X. Gong, X.W. Liu, Y.W. Yao, B.Y. Gao, Q.Y. Yue, Removal of lead(II) from aqueous solution by adsorption onto manganese oxide-coated carbon nanotubes, Sep. Purif. Technol. 58 (2007) 17–23.
[21] R.M. Cornell, U. Schwertmann, The Iron Oxides: Structure, Properties, Reactions, Occurences and Uses, second ed., Wiley-VCH Verlag GmbH & Co. KGaA, Weinheim, 2003.
[22] N. Jović-Jovičić, A. Milutinović-Nikolić, P. Banković, Z. Mojović, M. Žunić, I. Gržetić, D. Jovanović, Organo-inorganic bentonite for simultaneous adsorption of Acid Orange 10 and lead ions, Appl. Clay Sci. 47 (2010) 452–456.

[23] S. Yang, J. Li, Y. Lu, Y. Chen, X. Wang, Sorption of Ni(II) on GMZ bentonite: effects of pH, ionic strength, foreign ions, humic acid and temperature, Appl. Radiat. Isot. 67 (2009) 1600–1608.
[24] O. Gok, A.S. Ozcan, A. Ozcan, Adsorption behavior of a textile dye of Reactive Blue 19 from aqueous solutions onto modified bentonite, Appl. Surf. Sci. 256 (2010) 5439–5443.
[25] S. Honga, C. Wena, J. Hea, F. Gana, Y. Shan Ho, Adsorption thermodynamics of Methylene Blue onto bentonite, J. Hazard. Mater. 167 (2009) 630–633.
[26] O.N. Krasnobaeva, I.P. Belomestnykh, G.V. Isagulyants, T.A. Nosova, T.A. Elizarova, T.D. Teplyakova, D.F. Kondakov, V.P. Danilov, Synthesis of complex hydroxo salts of magnesium, nickel, cobalt, aluminum, and bismuth and oxide catalysts on their base, Russ. J. Inorg. Chem. 52 (2) (2007) 141–146.
[27] O.N. Krasnobaeva, I.P. Belomestnykh, G.V. Isagulyants, T.A. Nosova, T.A. Elizarova, D.F. Kondakov, V.P. Danilov, Chromium, vanadium, molybdenum, tungsten, magnesium, and aluminum hydrotalcite hydroxo salts and oxide catalysts on their base, Russ, J. Inorg. Chem. 54 (4) (2009) 495–499.
[28] J. Rouquerol, F. Rouquerol, K.S.W. Sing, Adsorption by Powders and Porous Solids: Principles, Methodology and Applications, Academic Press, San Diego, USA, 1999.
[29] T.K. Naiya, A.K. Bhattacharya, S.K. Das, Adsorption of Cd(II) and Pb(II) from aqueous solutions on activated alumina, J. Colloid Interface Sci. 333 (2009) 14–26.
[30] A.K. Meenaa, K. Kadirvelu, G.K. Mishraa, C. Rajagopal, P.N. Nagar, Adsorption of Pb(II) and Cd(II) metal ions from aqueous solutions by mustard husk, J. Hazard. Mater. 150 (2008) 619–625.
[31] D. Xu, X.L. Tan, C.L. Chen, X.K. Wang, Adsorption of Pb(II) from aqueous solution to MX-80 bentonite: effect of pH, ionic strength, foreign ions and temperature, Appl. Clay Sci. 41 (2008) 37–46.
[32] M. Sekar, V. Sakthi, S. Rengaraj, Kinetics and equilibrium adsorption study of lead(II) onto activated carbon prepared from coconut shell, J. Colloid Interface Sci. 279 (2004) 307–313.
[33] M. Momčilović, M. Purenović, A. Bojić, A. Zarubica, M. Ranđelović, Removal of lead(II) ions from aqueous solutions by adsorption onto pine cone activated carbon, Desalination (2011), doi:10.1016/j.desal.2011.03.013.
[34] V.J. Inglezakis, M.A. Stylianou, D. Gkantzou, M.D. Loizidou, Removal of Pb(II) from aqueous solutions by using clinoptilolite and bentonite as adsorbents, Desalination 210 (2007) 248–256.
[35] H. Chen, J. Zhao, G. Dai, J. Wu, H. Yan, Adsorption characteristics of Pb(II) from aqueous solution onto a natural biosorbent, fallen *Cinnamomum camphora* leaves, Desalination 262 (2010) 174–182.
[36] Q. Liu, Y. Liu, Distribution of Pb(II) species in aqueous solutions, J. Colloid Interface Sci. 268 (2003) 266–269.
[37] M. Kosmulski, Compilation of PZC and IEP of sparingly soluble metal oxides and hydroxides from literature, Adv. Colloid Interface Sci. 152 (2009) 14–25.
[38] S.V. Krishnan, I. Iwasaki, Heterocoagulation vs. surface precipitation in a quartz-$Mg(OH)_2$ system, Environ. Sci. Technol. 20 (1986) 1224–1229.
[39] D.G. Strawn, D.L. Sparks, The use of XAFS to distinguish between inner- and outer-sphere lead adsorption complexes on montmorillonite, J. Colloid Interface Sci. 216 (1999) 257–269.
[40] K.L. Mercer, J.E. Tobiason, Removal of arsenic from high ionic strength solutions: effects of ionic strength, pH, and preformed versus in situ formed HFO, Environ. Sci. Technol. 42 (2008) 3797–3802.